Design and Modeling of a Multi-segment Steerable Sheath for Single-port Endoscopic Procedures

Jiaole Wang[1], Pierre E. Dupont[1]

[1]Boston Children's Hospital, Harvard Medical School, Boston, USA

jiaole.wang@childrens.harvard.edu (DOI10.31256/HSMR2019.23)

INTRODUCTION

This paper presents a steerable continuum sheath for use in single-port minimally invasive procedures. The sheath is designed to not only deliver multiple robotic arms through its working channels or lumens, but also to be steerable such that the endoscope can follow a curved path to the surgical site (see Fig. 1). The goal is to provide a means to increase the dexterity that can be achieved by multi-armed straight endoscopic systems such as proposed in [1, 2].

Several methods for steering multi-armed endoscopic systems have been previously proposed: a push-pull rod-driven mechanism was described in [3], and a concentric-tube mechanism was introduced in [4]. The push-pull rod-driven mechanism is effective in producing significant bending of the sheath, however, this approach requires reserving a portion of the cross section for routing of the rods or tendons. The challenge of designing a steerable sheath using concentric tubes [5] is that the maximum curvature of the sheath is limited by its relatively large outer diameter. The alternative approach of this paper is to produce bending of the sheath using precurved working channels. The smaller diameter of the working channels with respect to the overall sheath means that significantly larger precurvatures can be used with this approach. This idea, first introduced in [6] for a single-section sheath, is extended and demonstrated here for two-section sheaths.

Articulation of the sheath is achieved by using one or more precurved superelastic tubes lining the working channels used for arm delivery. These tubes can accomplish shape change of the sheath through any combination of pushing, pulling and rotation. The sheath can be modeled using Cosserat rod theory to describe each working channel. These rod models are constrained along their length by a central backbone that can also be modeled as a Cosserat rod. The specific case of 2-armed 2-segment sheath is investigated here. Each working channel is comprised of a single precurved tube and actuation is achieved solely by rotation of the two precurved tubes relative to the central backbone. Simulation and experiment are used to investigate the concept and to evaluate the kinematic model.

MATERIALS AND METHODS

The main structure of a single-segment two-channel steerable sheath is shown in Fig. 1. The two pre-curved tubes lining the working channels can be rotated at the proximal end with respect to the central backbone of the sheath to produce sheath bending. A multi-segment steerable sheath can be formed when there are multiple precurved tubes telescopically inserted together. It is noted that the tool-mounted arms delivered through these working channels can be actuated by tendons, rods, concentric tubes, etc. As depicted, disks spaced along the length of the sheath are attached to a central backbone. These disks constrain the relative positions of the channel tubes. Since the channel diameters are typically at least a factor of two smaller than the sheath diameter, the maximum precurvature is proportionally larger than what could be achieved with a sheath constructed from concentric tubes. This design is also spatially efficient by utilizing the working channels, traditionally passive elastic components, for actuation.

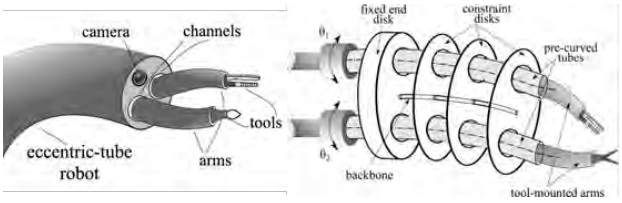

Fig. 1. Steerable endoscopic sheath actuated by rotation of two precurved tubes forming the working channels for the two robotic arms.

Kinematic modeling consists of solving for the shape of the backbone and precurved tubes by integrating a set of differential equations. The shapes of backbone and tubes is represented by $\mathbf{p}_i(s_i)$, where $s_i \in [0, \ell_i]$ is the independent arc length variable, ℓ_i is the tube length. The orientation of the body local frame is represented by a rotation matrix $\mathbf{R}_i(s_i)$which is defined as a Bishop frame moving along the tubes. The shape of the entire tube can be obtained by integrating $\dot{\mathbf{p}}_i(s_i) = \mathbf{R}_i(s_i)\mathbf{e}_3$ and $\dot{\mathbf{R}}_i(s_i) = \mathbf{R}_i(s_i)\hat{\mathbf{u}}_i$ from the proximal end to the distal end, where $\mathbf{u}_i(s_i)$ is defined as the local curvature and $\hat{\mathbf{u}}_i$ is a skew-symmetric matrix derived from $\mathbf{u}_i$.

For a single-segment sheath as introduced in [6], each precurved tube and the central backbone can be modeled as Cosserat rods subject to forces and moments applied to each other via the disks. The disks divide the tubes into sections over which integration is performed. According to Cosserat rod theory, the differential equation of curvature is given by

$$\dot{\mathbf{u}}_i = -\mathbf{K}_i^{-1}[\hat{\mathbf{u}}_i\mathbf{K}_i(\mathbf{u}_i - \mathbf{u}_i^*) + \mathbf{e}_3\mathbf{R}_i^{\mathrm{T}}\mathbf{n}_i], \quad (1)$$

where the subscript $i \in [0, \cdots, n]$ denotes the index for the tubes, and $i = 0$ stands for the backbone. The internal force is denoted as $\mathbf{n}_i$, and $\dot{\mathbf{n}}_i = 0$ since there is

no external force exerted on the tubes between disks. The tube stiffness is denoted as $\mathbf{K}_i = \mathrm{diag}([K_b, K_b, K_t])$, where K_b, K_t are the bending and torsional stiffness of the tube.

For the multi-segment sheath, the modeling of the central backbone is the same as for a single segment. With the working channel tubes, however, one must consider the relative twisting of the tubes. This matches the case of concentric tube robot modeling introduced in [5] since the telescopically aligned tubes can twist independently. This twist can be captured by the relative angle α_{ij} in local Z-axis with respect to the innermost (j=1)-th tube, where i and j are indexes for arm and tube, respectively. Therefore, the orientation of the j-tube of i-arm is $\mathbf{R}_{ij}(s) = \mathbf{R}_{i1}(s)\mathbf{R}_{\alpha_{ij}}(s)$ and $\mathbf{R}_{\alpha_{ij}}(s) = \exp(\alpha_{ij}(s)\hat{\mathbf{e}}_3)$. After some manipulation, the derivative of α_{ij} in terms of local torsional curvature $\mathbf{u}_{ij}(s)|_z$ is found to be $\dot{\alpha}_{ij}(s) = \mathbf{u}_{ij}(s)|_z - \mathbf{u}_{i1}(s)|_z$. As a result, the arm curvature can be integrated separately from bending and torsion. The bending curvature of i-th arm can be found as the 1-st tube as

$$\dot{\mathbf{u}}_{i1}|_{x,y} = -\mathbf{K}_i^{-1}\Big[\sum_{j=1}^{m}[\hat{\mathbf{u}}_{i1}\mathbf{K}_{ij}(\mathbf{u}_{i1} - \mathbf{R}_{\alpha_{ij}}\mathbf{u}_{ij}^*) - \dot{\alpha}_{ij}\mathbf{K}_{ij}\mathbf{R}_{\alpha_{ij}}\hat{\mathbf{e}}_3\mathbf{u}_{ij}^*] + \hat{\mathbf{e}}_3\mathbf{R}_{i1}^{\mathrm{T}}\mathbf{n}_i]\Big|_{x,y}, \quad (2)$$

where the external forces applied to each tube can be expressed collectively as $\mathbf{n}_i(s) = \sum_{j=1}\ \mathbf{n}_{ij}(s)$ and collective stiffness is defined as $\mathbf{K}_i = \sum_{j=1}\ \mathbf{K}_{ij}$. Assuming no friction between tubes and disks, the differential equation for the torsional curvature of each tube takes the form

$$\dot{\mathbf{u}}_{ij}|_z = \frac{K_{bij}}{K_{tij}}[\mathbf{u}_{ij}^*|_x(\mathbf{u}_{i1}|_x\sin(\alpha_{ij}) - \mathbf{u}_{i1}|_y\cos(\alpha_{ij})) + \mathbf{u}_{ij}^*|_y(\mathbf{u}_{i1}|_x\cos(\alpha_{ij}) + \mathbf{u}_{i1}|_y\sin(\alpha_{ij}))]. \quad (3)$$

All differential equations are integrated simultaneously along the length of tubes to calculate the shape of each working channel. The boundary conditions, the compatibility condition imposed by disks, and solution approach are the same as those in [6]. Convergence in simulation is assumed when compatibility error is less than 0.6mm.

Table I. Prototype Parameters.
(Fig. 2-3 Parameters / Fig. 4 parameters)

	Segment 1	Segment 2	Backbone
Disk spacing (mm)	8		
Length (mm)	35 / 55	35 / 50	64 / 100
Radius of curvature (mm)	83.33 / 26.79	93.33 / 34.29	∞
Outer diameter (mm)	2.5 / 1.875	2.8 / 2.4	0.762mm
Inner diameter (mm)	2.2 / 1.6	2.6 / 2.0	--

RESULTS

Two 2-section steerable sheath prototypes were built as shown in Figs. 2-4 using the parameters of Table I. Initial validation of the model was performed by visual comparison of simulated and experimental shapes as shown in Fig. 3 for the low-curvature prototype. For this design, the model converged for a broad range of initial conditions while for the high curvature design, convergence was sensitive to initial conditions. Future work will focus on model solution techniques and calibration.

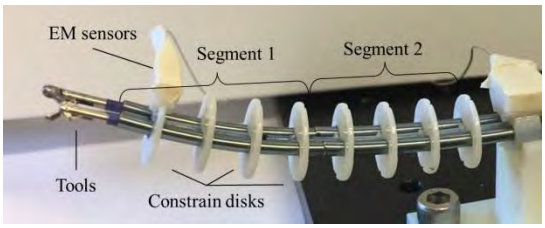

Fig. 2. Two-section sheath prototype accommodating two arms.

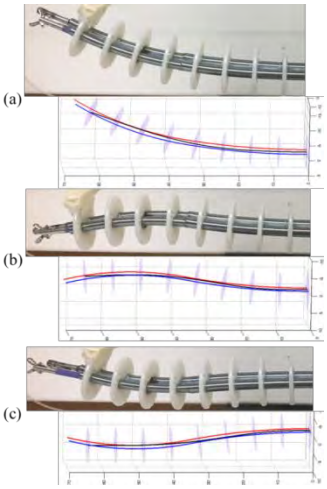

Fig. 3. Comparison of experimental and simulated shapes of low curvature tubes. Black curve is central backbone, blue and red curves are working channels corresponding to the left and right arms.

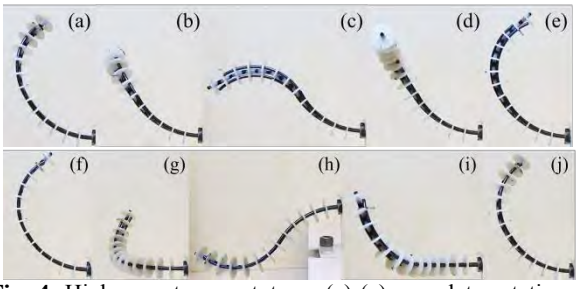

Fig. 4. High-curvature prototype. (a)-(e) complete rotation of distal section. (f)-(h) complete rotation of proximal section.

ACKNOWLEDGEMENTS

This work was supported by NIH grant R01NS099207.

REFERENCES

[1] H. Azimian *et al*. A Dual-arm Robotic Neuroendoscope: Early Results, *In HSMR*, 2016.
[2] R. J. Hendrick *et al*. Hand-held transendoscopicrobotic manipulators: A transurethral laser prostatesurgery case study, *Int*. *J*. *Robot*. *Res*. , 2015.
[3] N. Sarli *et al*. Preliminary Porcine In Vivo Evaluation of a Telerobotic System for Transurethral Bladder Tumor Resection and Surveillance, *J*. *Endourology*, 2018.
[4] Z. Mitros *et al*. Mechanics Modelling of Eccentrically Arranged Concentric Tubes, *In HSMR*, 2018.
[5] P. E. Dupont *et al*. Design and control of concentric-tube robots, *IEEE Trans*. *Robot*., 2010.
[6] J. Wang *et al*. Steering a multi-armed robotic sheath using eccentric precurved tubes, *In ICRA*, 2019.